ORIGINAL RESEARCH

Novel α-Actin Gene Mutation p.(Ala21Val) Causing Familial Hypertrophic Cardiomyopathy, Myocardial Noncompaction, and Transmural Crypts. Clinical-Pathologic Correlation

Andrea Frustaci, MD; Alessandro De Luca, PhD; Valentina Guida, PhD; Tommaso Biagini, PhD; Tommaso Mazza, PhD; Carlo Gaudio, MD; Claudio Letizia, MD; Matteo Antonio Russo, MD; Nicola Galea, MD; Cristina Chimenti, MD, PhD

***Background*—**Mutations of α-actin gene (ACTC1) have been phenotypically related to various cardiac anomalies, including hypertrophic cardiomyopathy and dilated cardiomyopathy and left ventricular (LV) myocardial noncompaction. A novel ACTC mutation is reported as cosegregating for familial hypertrophic cardiomyopathy and LV myocardial noncompaction with transmural crypts.

***Methods and Results*—**In an Italian family of 7 subjects, 4 aged 10 (II-1), 14 (II-2), 43 (I-4) and 46 years (I-5), presenting abnormal ECG changes, dyspnea and palpitation (II-2, I-4, and I-5), and recurrent cerebral ischemic attack (I-5), underwent 2-dimensional echo, cardiac magnetic resonance, Holter monitoring, and next-generation sequencing gene analysis. Patients II-2 and I-5 with ventricular tachycardia underwent a cardiac invasive study, including coronary with LV angiography and endomyocardial biopsy. In all the affected members, ECG showed right bundle branch block and left anterior hemiblock with age-related prolongation of QRS duration. Two-dimensional echo and cardiac magnetic resonance documented LV myocardial noncompaction in all and in I-4, I-5, and II-2 a progressive LV hypertrophy up to 22-mm maximal wall thickness. Coronary arteries were normal. LV angiography showed transmural crypts progressing to spongeous myocardial transformation with LV dilatation and dysfunction in the oldest subject. At histology and electron microscopy detachment of myocardiocytes were associated with cell and myofibrillar disarray and degradation of intercalated discs causing disanchorage of myofilaments to cell membrane. Next-generation sequencing showed in affected members an unreported p.(Ala21Val) mutation of ACTC.

***Conclusions*—**Novel p.(Ala21Val) mutation of ACTC1 causes myofibrillar and intercalated disc alteration leading to familial hypertrophic cardiomyopathy and LV myocardial noncompaction with transmural crypts. **(*J Am Heart Assoc*. 2018;7:e008068. DOI: 10.1161/JAHA.117.008068.)**

Key Words: familial hypertrophic cardiomyopathy • gene mutation • myocardial noncompaction

Hypertrophic cardiomyopathy (HCM; MIM #192600) is the most prevalent cardiomyopathy, affecting at least 1 in 500 people in the general population worldwide.[1,2]

HCM is characterized morphologically and defined by a hypertrophied, nondilated left ventricle in the absence of another systemic or cardiac disease that is capable of producing the magnitude of wall thickening evident.[2] More than 90% of HCM is inherited as an autosomal-dominant disease with variable expressivity and age-related penetrance. HCM occurs mainly because of mutations in genes encoding for the cardiac sarcomere. Around 70% of these mutations are in the sarcomere genes encoding for cardiac β-myosin heavy

From the Department of Cardiovascular, Respiratory, Nephrologic, Anesthesiologic and GeriatricSciences, Sapienza University, Rome, Italy (A.F., C.G., C.C.); Cellular and Molecular Lab, IRCCS L. Spallanzani, Rome, Italy (A.F., C.C.); Molecular Genetics Unit (A.D.L., V.G.) and Bioinformatics Unit (T.B., T.M.), Casa Sollievo della Sofferenza Hospital, IRCCS, San Giovanni Rotondo, Italy; Department of Internal Medicine, Center for Secondary Hypertension, Sapienza University, Rome, Italy (C.L.); IRCCS San Raffaele Pisana, and MEBIC Consortium, San Raffaele Rome Open University, Rome, Italy (M.A.R.); Department of Radiological, Oncological and Pathological Sciences, La Sapienza University, Rome, Italy (N.G.).

An accompanying Table S1 is available at http://jaha.ahajournals.org/content/7/4/e008068/DC1/embed/inline-supplementary-material-1.pdf

Correspondence to: Andrea Frustaci, MD, Department of Cardiovascular, Respiratory, Nephrologic, Anesthesiologic and GeriatricSciences, La Sapienza University, Viale del Policlinico 155, Rome 00161, Italy. E-mail: biocard@inmi.it

Received November 10, 2017; accepted November 28, 2017.

Clinical Perspective

What Is New?

- The identification of a novel p.(Ala21Val) ACTC1 gene mutation cosegregating for familial hypertrophic cardiomyopathy and left ventricular myocardial noncompaction with transmural crypts is reported.
- This single-point mutation of ACTC1 causes a composite structural change involving sarcomeres and intercalated discs.

What Are the Clinical Implications?

- Dysfunction of cytoplasmic α-actin causes a disanchorage of myofibrils to sarcolemmal membrane followed by myofibryllolysis and possibly cell death.
- Intercalated discs seem to be particularly involved by this mutation given that they appear irregular, and fragmented, favoring cell disconnection.

chain (*MYH7*; MIM *160760) and cardiac myosin binding protein C (*MYBPC3*; MIM *600958). Other sarcomeric genes involved in HCM are regulatory myosin light chain (*MYL2*; *160781), cardiac troponin T (*TNNT2*; MIM *191045), cardiac troponin I (*TNNI3*; MIM *191044), and actin (*ACTC1*; MIM *102540). Nonsarcomeric genes, such as genes encoding plasma membrane and mitochondrial proteins, as well as sarcomere adjacent Z-disc encoding genes, account for the other HCM cases.

Left ventricular (LV) noncompaction (LVNC), the most recently classified form of cardiomyopathy, is characterized by abnormal trabeculations in the left ventricle, most frequently at the apex. LVNC can be associated with LV dilation or hypertrophy, systolic or diastolic dysfunction, or both or various forms of congenital heart disease. Genetic inheritance arises in at least 30% to 50% of patients, and several genes that cause LVNC have been identified.[3,4] These genes seem generally to encode sarcomeric (contractile apparatus) or cytoskeletal proteins. Disrupted mitochondrial function and metabolic abnormalities were demonstrated to have a causal role, too.[5]

Recent literature has documented genetic evidence to prove LVNC and HCM as having causative genes, which are overlapping. Two separate autosomal-dominant LVNC families with mutations in the sarcomeric *MYH7* gene, known to be associated with HCM, restricted cardiomyopathy, and dilated cardiomyopathy, were described.[6,7] Monserrat et al[8] described another 5 families, 1 with LVNC and 4 with HCM with mutations in the *ACTC1* gene.

Other genes whose mutations have been implicated in both HCM and LVNC are *TPM1* and *MYBPC3*, encoding for tropomyosin 1 and cardiac myosin binding protein-C, respectively.[7–13]

In the following study, a novel p.(Ala21Val) *ACTC1* mutation manifesting with familial hypertrophic cardiomyopathy and myocardial noncompaction with transmural crypts, is reported. Combination of myocyte and myofibrillar disarray with degradation of intercalated discs because of abnormal anchorage of mutated ACTC1 protein to sarcolemmal membrane are shown to be at the base of the ultrastructural abnormality.

Methods

The data, analytical methods, and study materials will not be made available to other researchers for purposes of reproducing the results or replicating the procedure.

In an Italian family of 9 subjects (Figure 1), 1 dead at 50 years of age for cardiac arrest (I-1), 4 presented abnormal ECG changes, and 3 were symptomatic for palpitations and/or dyspnea. The oldest affected patient (II:5) presented also recurrent episodes of cerebrovascular transient ischemic attacks.

The 4 patients with ECG abnormalities (10 [III:1], 14 [III:2], 43 [II:4], and 46 [II:5] year-old male) had a 24 hs Holter monitoring that showed in the 14- (III:2) and 46-year-old subjects (II:5) runs of nonsustained ventricular tachycardia. The 4 subjects with ECG abnormalities had additionally an echocardiogram. The 2 patients with electrical instability had an implemental cardiac magnetic resonance and invasive cardiac study, including coronary angiography, LV angiography, and endomyocardial biopsy. All 7 subjects underwent a next-generation sequencing (NGS) gene analysis (Table).

Cardiac Studies

Institutional review board approval was obtained, according to the guidelines.

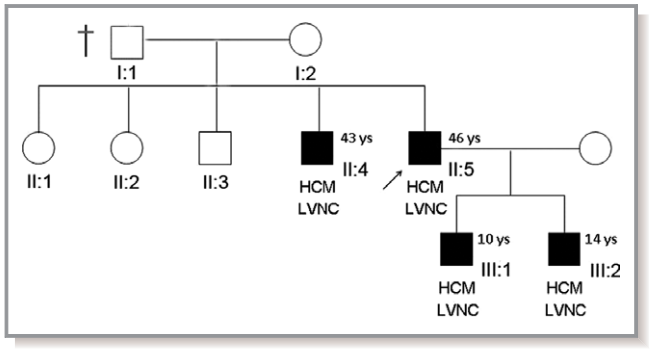

Figure 1. Pedigree of reported family. Squares and circles indicate male and female family members, respectively. Arrow indicates proband. Solid symbols are affected individuals. Ages refer to age of diagnosis. HCM indicates hypertrophic cardiomyopathy; LVNC, left ventricular noncompaction; ys, years.

Table. Clinical, Histological, and Molecular Data of the 4 Patients With LVNC

Patient	II-4	II-5	III-1	III-2
Age, y	43	46	10	14
ECG and Holter monitoring	RS, LAH, RBBB, VEB (Lown III)	AF, LAH, RBBB, RA, VEB (Lown IVA)	RS, LAH, incomplete RBBB, VEB (Lown II)	RS, LAH, incomplete RBBB, VEB (Lown IVA)
2D echocardiography	LV NC endocardial layer (NC/C ration ≥2) intertrabecular recesses MWT, 17 mm LVEDD, 53 mm EF, 55%	LV NC endocardial layer (NC/C ration ≥2) intertrabecular recesses, MWT, 22 mm LVEDD, 67 mm EF, 30%	LV NC endocardial layer (NC/C ration <2) intertrabecular recesses, MWT, 10 mm LVEDD, 36 mm EF, 63%	LV NC endocardial layer (NC/C ration <2) intertrabecular recesses, MWT, 12 mm LVEDD, 40 mm EF, 60%
Histology	Cardiomyocyte hypertrophy, disarray, moderate fibrosis	Cardiomyocyte hypertrophy, disarray, severe fibrosis	…	…
Electron microscopy	Myofibrillar disarray, myofibrillolysis, fragmented intercalated discs	Myofibrillar disarray, myofibrillolysis, fragmented intercalated discs	…	…
Gene mutation	ACTC 1 c.62C>T p(Ala21Val)	ACTC 1 c.62C>T p(Ala21Val) TTNc.28127C>G) p(T9376R)	ACTC 1 c.62C>T p(Ala21Val)	ACTC 1 c.62C>T p(Ala21Val) TTNc.28127C>G) p(T9376R)

ACTC indicates actin; C, compacted; EDD, end-diastolic diameter; EF, ejection fraction; FA, atrial fibrillation; LAH, left anterior hemiblock; LV, left ventricular; MWT, maximal wall thickness; NC, noncompacted; RA, repolarization abnormalities; RBBB, right bundle branch block; RS, synus rhythm; TTN, titin; VEB, ventricular ectopic beats.

Cardiac magnetic resonance exams have been perfomed on a 1.5 Tesla scanner (Avanto; Siemens Medical Solutions, Erlangen, Germany). Standard cardiac magnetic resonance protocol included: (1) Cine magnetic resonance images acquired during breath-holds in the short-axis, 2-chamber, and 4-chamber; (2) black blood T2-weighted short tau inversion recovery images on short-axis planes covering the entire left ventricle during 6 to 8 consecutive breath-holds for myocardial edema detection; (3) late gadolinium-enhanced imaging performed 15 minutes after injection of 0.2 nmol/kg of gadoteratemeglumine (gadolinium-DOTA, Dotarem; Guerbet, Paris, France), and signal intensity value 2 SDs above the mean signal intensity of the remote normal myocardium was considered suggestive for myocardial fibrosis.

Cardiac catheterization, selective coronary with LV angiography, and endomyocardial biopsy followed patients' written informed consent. Biopsies (5 samples each patient) were performed in the septal-apical region of the left ventricle.

Histology and Electron Microscopy

Endomyocardial biopsies were fixed in 10% buffered formalin and paraffin embedded. Sections (5 μm) were stained with hematoxylin and eosin, Masson thrichrome, and Miller's Elastic Van Gieson. For transmission electron microscopy, endomyocardial biopsies were fixed by 2.5% glutaraldehyde solution in phosphate buffer (0.1 mol/L, pH 7.3 at cold), then postfixed in osmium tetroxide and processed following a standard schedule for embedding in Epon resin. Semithin plastic sections were stained at warm with AzurII and basic fucsin. Ultrathin sections were stained with uranyl acetate and lead hydroxide. A Philips (CM-10; Philips, Best, The Netherlands) transmission electron microscope was used for observation and photographic analysis.

NGS and Structural Interpretation of Variants

Genomic DNA was isolated from peripheral blood using Macherey-Nagel NucleoSpin blood extraction kit (Macherey-Nagel, Duren, Germany). Targeted enrichment was performed using TruSight Cardio Sequencing Kit (Illumina, San Diego, CA). This target panel includes 174 genes with known associations to 17 different inherited cardiac conditions (see Table S1 for the list of genes included in the gene panel; Pua et al).[14] Captured libraries were loaded onto a MiSeq sequencing platform (Illumina, San Diego, CA).

Sequences (aka reads) were analyzed using a custom software pipeline. In brief, paired-end reads were aligned to the GRCh37/hg19 reference genome by Bowtie 2 (version 2.3.0). BAM files were sorted by SAM tools (version 1.3.2) and purged from candidate PCR duplicates using Mark Duplicates from the Picard suite (version 2.9.0). The alignment process was optimized by the local realignment and base-quality-score recalibration functions, as implemented in the Genome Analysis Toolkit (GATK 3.5). To confer higher confidence, both reads and alignments underwent an extensive evaluation of the base-per-position and mapping-per-read quality scores. Reads with mapping quality scores lower than 20 or with more than one half nucleotides with quality scores less than 30 were filtered out. The GATK's Haplotype Caller was used to

identify single-nucleotide polymorphisms and insertions/deletions. Genetic variants were annotated by ANNOVAR and subjected to filtering. In particular, only novel or rare exonic and splicing variants were considered. Thus, these variants exhibited an allele frequency lower than 1% in the general population, as from dbSNP 149 (https://www.ncbi.nlm.nih.gov/projects/SNP/), GO-ESP (http://evs.gs.washington.edu/EVS/) and ExAC (http://exac.broadinstitute.org/). The pathogenicity of these variants was assessed in silico using 13 pathogenicity predictors (eg, SIFT, PolyPhen 2, Mutation Assessor and CADD, and thermodynamically). In particular, the thermodynamic stability of the wild-type or mutant proteins was investigated using the FoldX algorithm. It computed the total energy of proteins, as a proxy of their overall stability, and the Van der Waals inter-residue clashes, as energy penalization factors. Thus, the 3-dimensional structures of both proteins were minimized, namely all the side chains were slightly moved in order to reduce the Van der Waals' clashes. It was run with standard parameters on a system modeled on a template of the rabbit skeletal muscle actomyosin rigor complex (Protein Data Bank ID: 5h53). A stand-alone version of FoldX is available from http://foldx.crg.es (Schymkowitz et al).[15] Potentially harmful variants were finally prioritized considering familial segregation. Variants identified using NGS were validated by Sanger sequencing and segregation analysis using the ABI BigDye Terminator Sequencing Kit v.3.1 (Life Technologies, Carlsbad, CA) and an ABI 3130XL automated sequencer.

Results

Cardiac Studies

ECG in the 4 affected members showed similar changes consisting in right bundle branch block and left anterior hemiblock with increased QRS duration in the oldest patient, associated to negative T waves in the anterolateral leads. Ventricular ectopic beats were documented in patients II-4, II-5, and III-2. In patients III-2 and II-5 runs of nonsustained ventricular tachycardia were also registered.

Two-dimensional echocardiogram showed prominent trabeculations with evidence of irregular endocardial surface in all 4 affected family members. Particularly in II-4 and II-5 patients, deep endocardial recesses were documented with color Doppler, meeting the echocardiographic diagnostic criteria for LVNC (ie, noncompaction/compaction ratio $\geq$2).[16] A remarkable LV hypertrophy with an LV maximal wall thickness of 12-, 17-, and 22-mm thickness was observed in patients II-4, II-5, and III-2, respectively. The youngest 10-year-old boy (II-1) had normal cardiac wall thickness, dimensions, and function. The II-5 had also a dilated (end-diastolic diameter, 67 mm) and severely hypokinetic (ejection fraction, 30%) left ventricle. Cardiac magnetic resonance showed in the III-2 symmetric mild LV hypertrophy diffusely involving all myocardial segments with a maximal wall thickness of 12 mm (Figure 2). In particular, cine steady-state free precession images acquired on midventricular short-axis (Figure 2A and 2B) and vertical long-axis (Figure 2C and 2D) views showed trabeculated noncompacted myocardium involving anterior and lateral walls, and deep transmural crypts located at the basal inferior LV wall. No areas of gadolinium enhancement have been detected on late gadolinium-enhanced inversion recovery imaging.

In the II-5 patient, cine steady-state free precession images showed deep myocardial crypts penetrating almost the entire thickness of the myocardium, involving almost all segments, hyperthophy of basal septum (maximal wall thickness, 22 mm), and highly trabeculated midapical anterolateral wall as commonly observed in noncompaction myocardium (Figure 3A through 3C). Late gadolinium-enhanced inversion recovery short-axis image showed diffuse enhancement of anterolateral wall consistent with diffuse interstitial myocardial fibrosis (Figure 3D).

Coronary angiography obtained in the III-2 and II-5 affected members was normal. In these patients, LV angiography confirmed the presence of transmural crypts (Figures 2 and 3E, 3F) particularly prominent in the oldest patient where they assumed a spongeous conformation (Figure 3E and 3F) becoming the likely source of cerebral thromboembolism.

Histology and Electronmicroscopy

At histology, cardiomyocytes were hypertrophied up to 60 μm in diameter at nuclear level and often in total disarray (Figures 2 and 3G). Myocytes were diffusely separated by unendotheliolized spaces and channels of various width. These changes were more prominent in the I-5 patient where a remarkable interstitial and replacement fibrosis was also documented. At ultrastructural examination diffuse myofibrillar disarray was present. The intercalated discs were diffusely irregular, fragmented (Figure 2H), and often detached (Figure 3H), being connected with areas of myofibrillolysis, likely attributed to disanchorage of mutated cytoplasmic alpha-actin.

Molecular Studies

The affected family members having LVNC associated with HCM (I:5 and II:2) were mutation scanned using the targeted NGS TruSight Cardio Kit panel including 174 genes involved in inherited cardiac conditions.[14] Among a total of 32 000 variants identified by NGS analysis, after selection and prioritization filtering, 2 variants, both confirmed by Sanger sequencing, were found to be shared by both individuals, 1 in

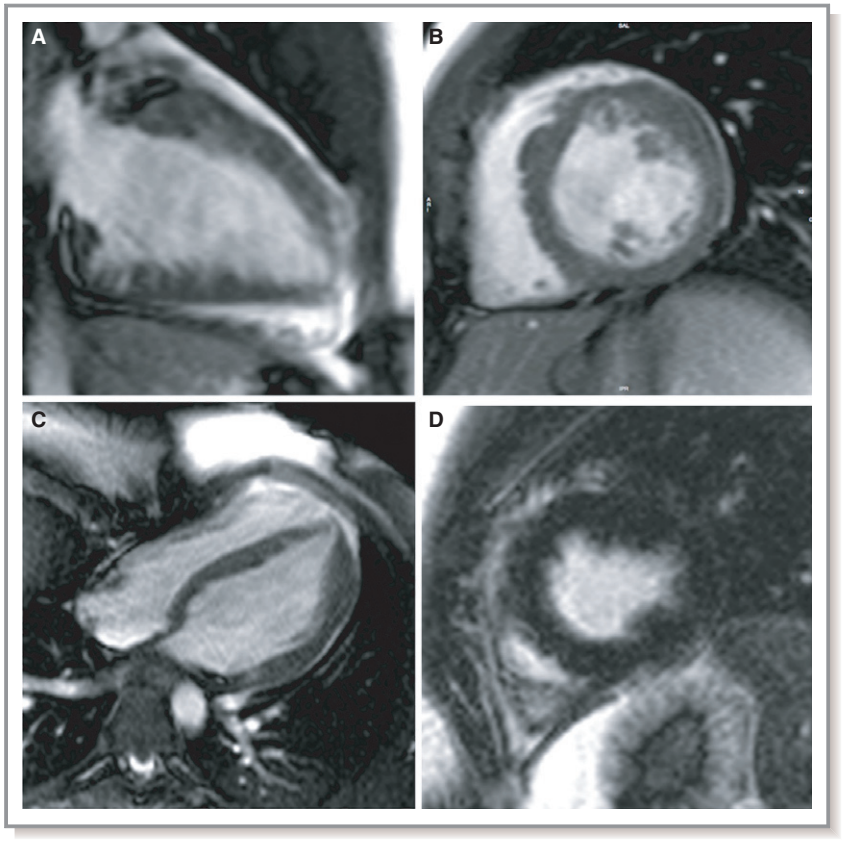

Figure 2. Magnetic resonance, histological, and ultrastructural characteristics of patient III-2 with α-actin gene mutation p.(Ala21Val). Cine steady-state free precession image acquired on vertical long axis (A) midventricular short-axis (B) and horizontal long-axis (C) views show diffuse and symmetric mild left ventricular hypertrophy, mostly distributed at basal anterior wall (maximal wall thickness, 12 mm) and apical lateral wall, trabeculated noncompacted myocardium involving anterior and lateral walls, and deep transmural crypts located at basal inferior LV wall (arrowheads). No areas of gadolinium enhancement have been detected on late gadolinium-enhanced inversion recovery imaging (D). E and F, Represents diastolic and systolic frames of LV angiography showing diffuse transmural crypts with preserved LV function. G and H, LV endomyocardial biopsy showing hypertrophy with disarray of myocardiocytes with cell separated by unendothelialized large and deep spaces (c=channels). At high magnification (H) detail of 2 myocardiocytes in a region close to their intercalated disc. The organization of sarcomeric filaments appears variously disordered, possibly attributed to the mutated nonsarcomeric actin, which normally contributes to the physiological interactions between sarcomeric actin and anchorage system of Z-disc associated to the intercalated disc. Bar represents 10 μm. LV indicates left ventricular.

the *ACTC1* gene [NM_005159.4:c.62C>T;p.(Ala21Val)], encoding for the skeletal muscle alpha-actin, and the other in the *TTN* gene [NM_001267550:c.28127C>G;p.(Tyr9376-Arg)], encoding for Titin, a giant muscle protein expressed in the cardiac and skeletal muscles. *ACTC1* p.(Ala21Val) variant alters a highly conserved amino acid, up to Baker's yeast, located within the actin-like domain of the protein. It is not reported by public single-nucleotide polymorphism databases (1000 genomes, ExAC) and is deemed deleterious by various in silico prediction programs (SIFT, score=0.03; PolyPhen2, score=0.85; MutationTaster, P=1; CADDphred=24.2). p.(Tyr9376Arg) variant is a rare *TTN1* allele reported with a frequency of C=0.00005/6 in the ExAC population database (rs749875409). No protein conservation data are available for this variant, which is also reported as a variant with uncertain significance in the ClinVar database, a public archive of reports of clinical significance of variants (https://www.ncbi.nlm.nih.gov/clinvar/). To further prioritize the 2 variants, their patterns of segregation were analyzed by Sanger sequencing in available family members (II:1, II:2, II:3, II:4, and III:2). Sequence analysis confirmed segregation of the *ACTC1* p.(Ala21Val) variant with the disease in 2 further affected

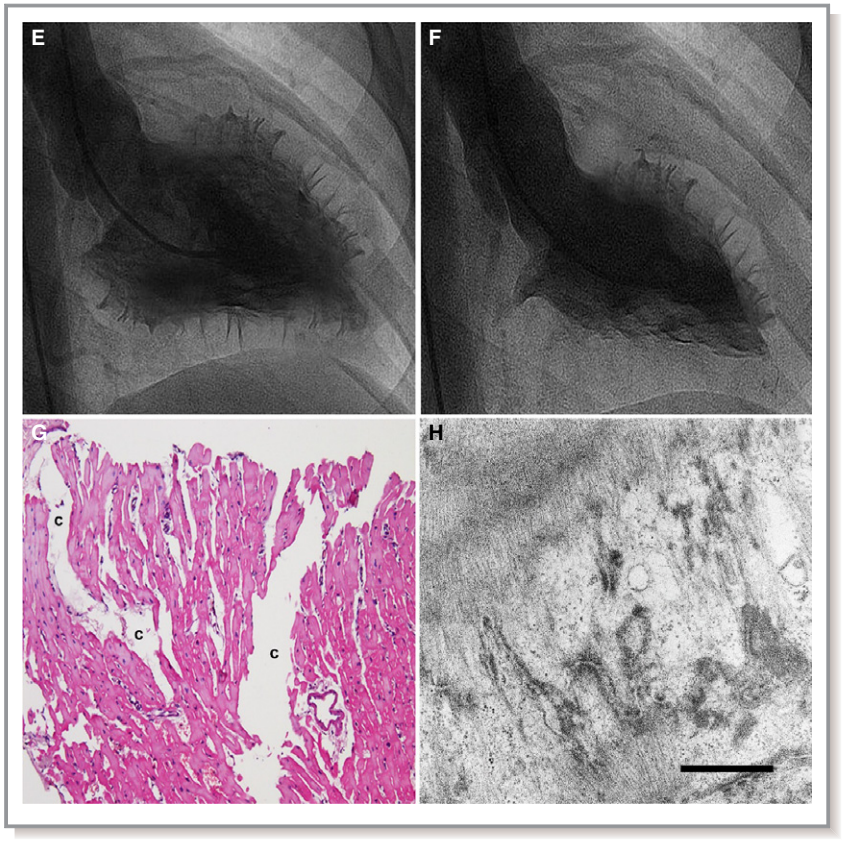

Figure 2. Continued.

family members (II:4, III:1), whereas *TTN* variant p.(Tyr9376-Arg) was found not to segregate with the disease phenotype. Therefore, we propose that *ACTC1* p.(Ala21Val) is the disease-causing mutation of this family. To further confirm the pathological effects of *ACTC1* p.(Ala21Val) missense variant, its thermodynamic impact on the stability of the overall 3-dimensional structure of ACTC1 was assessed by the FoldX algorithm (Figure 4). Following free energy calculations, ΔG_{mut}=213.85 kcal/mol and ΔG_{wt}=211.49 kcal/mol, we estimated a $\Delta\Delta G$ increase, after mutation, of 2.36 kcal/mol ($\pm$0.005 kcal/mol), which is compatible with the highly destabilizing character hypothesized for the variant under examination.

Treatment and Follow-up

The three patients with preserved cardiac dimensions and function were treated with bisoprolol (2.5 mg daily for the III:1 and III:2; 5 mg daily for I:4). The II:5 with cardiac dilatation and severe dysfunction received carvedilol 25 mg tid in addition to amiodarone 200 mg daily, diuretics and angiotensin-converting enzyme inhibitors. Warfarin was introduced because of recurrent cerebrovascular transient ischemic attacks. He also underwent an implantable cardioverter defibrillator implantation and was suggested for cardiac transplantation.

The first 3 patients were followed for a 5-year time. Clinical conditions were stable; no major arrhythmias were recorded at repeated (every 3 months) Holter monitoring; LV wall thickness, dimension, and function remained unchanged.

Discussion

A novel α-actin gene mutation p.(Ala21Val) causing familial HCM, myocardial noncompaction, and transmural crypts is reported on. This *ACTC1* mutation is exceedingly rare and was not detected in over 126 000 individuals in the ExAC database. Moreover, a range of mutation analysis approaches (SIFT, PolyPhen2, MutationTaster, and CADDphred), homology studies, and protein modeling all suggest that the p.(Ala21Val) mutation is pathogenic. Furthermore, the p.(Ala21Val) mutation strongly cosegregates with the disease, providing additional support for its pathogenicity. *ACTC1* gene mutations have been phenotypically related with diverse cardiac anomalies, including dilated cardiomyopathy,[17] hypertrophic cardiomyopathy,[18–20] myocardial noncompaction,[8,21] and congenital heart defects, in particular atrial septal defect.[22]

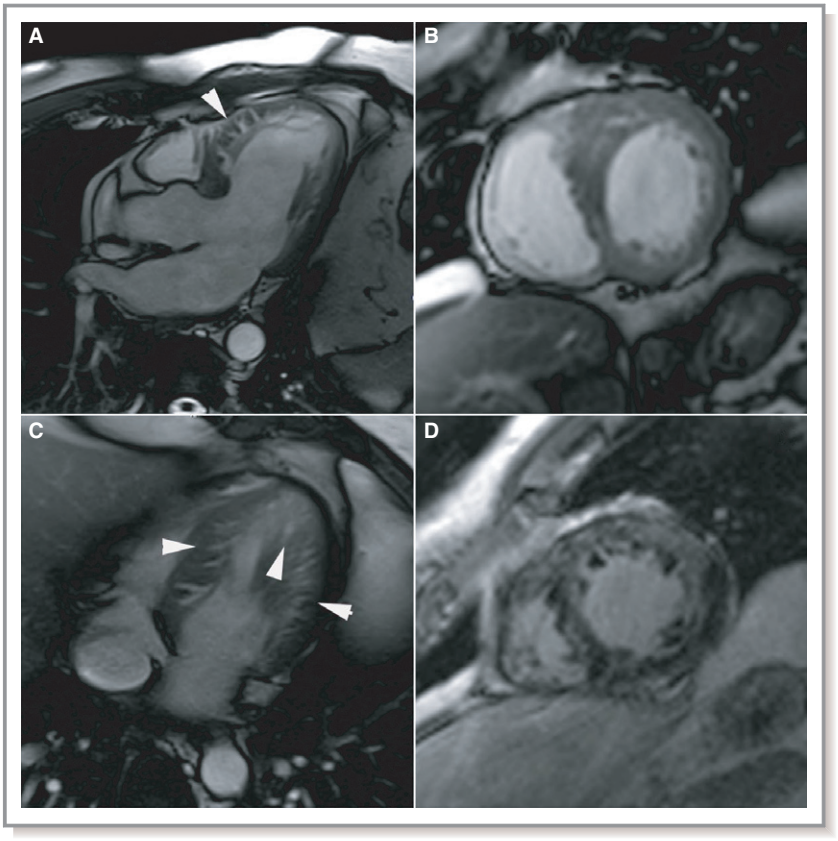

Figure 3. Magnetic resonance, histological, and ultrastructural characteristics of patient II-5 with α-actin gene mutation p.(Ala21Val). Cine steady-state free precession images acquired on 3-chamber (A), short-axis (B), and 4-chamber (C) views show deep myocardial crypts (arrowheads) penetrating almost the entire thickness of myocardium, involving almost all segments, hypertrophy of basal septum (maximal wall thickness, 22 mm), and highly trabeculated midapical anterolateral wall as commonly observed in noncompaction myocardium. Late gadolinium-enhanced inversion recovery short-axis image (D) shows diffuse enhancement of anterolateral wall consistent with diffuse interstitial fibrosis. E and F, LV angiography showing LV dilation and dysfunction associated with spongeous conformation of LV myocardium. G, LV endomyocardial biopsy showing severe hypertrophy with disarray of cardiomyocytes separated by large unendothelialized channels (c=channels). H, TEM at low magnification of the final niche of the abnormal invaginations among myocardiocytes, which characterize the "spongy" zone of the myocardium. The compact zone is clearly defined by the presence of junctional complexes of the intercalated disc. Myocardiocytes (lower part of the picture) can show large areas of myofibrillolysis. Bar represents 10 μm. LV indicates left ventricular; TEM, transmission electron microscopy.

To our knowledge, this is the first report in which a sarcomeric gene mutation is found to cosegregate with both HCM and LVNC in multiple family members, suggesting that *ACTC1* p.(Ala21Val) mutation causes a high penetrance for both HCM and LVNC.

Genotype-phenotype correlations within the *ACTC1* mutation spectrum are not unexpected, for example, *ACTC1* mutations resulting in congenital heart defects (essentially atrial septal defects) are restricted to the first half of the protein (from residue Met^{84} to residue Met^{178}),[23] whereas beyond residue Met^{178}, all reported *ACTC1* mutations are found to result in cardiomyopathies[17–20] with an unusual prevalence of noncompaction or hypertrophied apex.

In 2 patients with ACTC1 mutation and pronounced ventricular arrhythmias, an additional mutation of TTN gene has been found, suggesting that it might have contributed to the arrhythmic phenotype. On the other hand, TTN mutation has been associated with arrhythmic cardiomyopathies.[24]

Diagnosis of HCM has been supported by an age-related progressive thickening of LV walls associated to severe hypertrophy with disarray of myocardiocytes at histology.

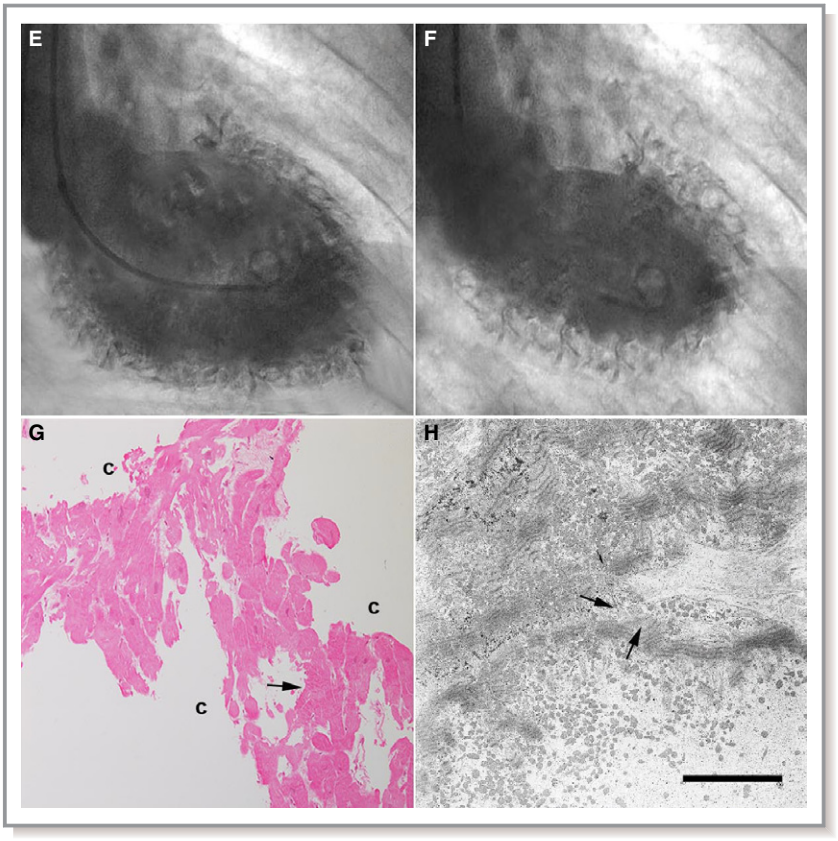

Figure 3. Continued.

Myocytes were also found frequently separated by unendotheliolized spaces of various width, suggesting the coexistence of myocardial noncompaction. Crypts, defined as narrow, deep blood-filled endocardial invaginations within the myocardium, were transmural and diffusely distributed along the left ventricle if compared with isolated HCM and healthy volunteers where they are of limited number and depth.[25,26] It may be that these architectural abnormalities, first described at postmortem with HCM[27–29] and recently recognized by cardiac magnetic resonance in 5% of normal, 4% of HCM, and 61% of genotype-positive phenotype-negative (prehypertrophic) HCM,[21,22] may contribute to disease progression when diffusely associated to myocardial noncompaction.

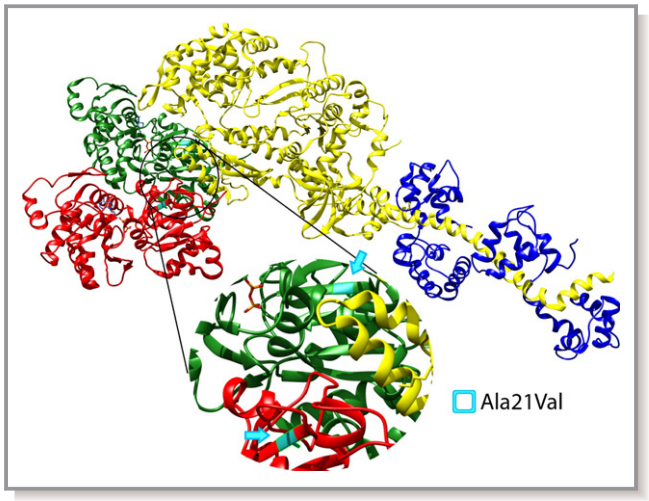

Figure 4. Location of Ala^{21} in the tridimensional structure of the actin–myosin binding module. Docking of S1 myosin domain (yellow) onto actin showing that S1 interacts with 2 actin molecules (green and red). Ala^{21} (colored in cyan and highlighted by arrows) is part of the actin core domain and is nearby the binding site with ATP.

What appears from gene analysis by NGS of affected and nonaffected members of our family is that the previously unreported p.(Ala21Val) missense mutation of *ACTC1* is associated with multiple structural changes involving sarcomeres and their anchorage to sarcolemmal membrane. Indeed, this variant alters a highly conserved amino acid located within the actin-like domain of the protein. In addition, the thermodynamic studies of mutated protein obtained in our cases suggest that this mutation is highly destabilizing conferring to the protein a pathogenic impact.

Structural consequences of the mutated protein are delineated by histological and ultrastructural examination of LV endomyocardial biopsies obtained in 2 affected members. Specifically, mutation of sarcomeric α-actin is followed by

fibrils disarray and hypertrophy with disarray of myocardiocytes. Dysfunction of cytoplasmic α-actin causes a disanchorage of myofibrils to the sarcolemmal membrane followed by myofibryllolysis and, possibly, cell death. Intercalated discs seem to be particularly involved by this mutation given that they appear irregular, and fragmented, favoring cell disconnection.

Clinical implications have been reported as arrhythmic early in life, hypertrophic with diastolic dysfunction, and dyspnea up to middle age evolving toward cardiac dilatation and dysfunction in the fifth decade of life. Spongeous transformation of LV myocardium and heart failure eventually predispose to cardiac thrombus formation and systemic embolization.

As far as therapy is concerned, early recognition of this entity and treatment with beta-blockers may control cardiac arrhythmias reducing cellular stress and perhaps limit the disease progression. Anticoagulation may be required in the occurrence of heart failure and/or thromboembolic events.

In conclusion, p.(Ala21Val) mutation of *ACTC1* is a novel pathogenic variant giving rise to a complex structural change in human myocardium, including HCM, myocardial noncompaction, and transmural crypts. This results in electrical instability, cardiac dilatation, and failure requiring heart transplantation in the fifth decade of life.

Sources of Funding

The study was supported by the “Ateneo La Sapienza” grant C26H15H9LP “Differential mutated gene expression causing cardiomyocyte phenotype variation in human hypertrophic cardiomyopathy.”

Disclosures

None.

References

1. Maron BJ, Towbin JA, Thiene G, Antzelevitch C, Corrado D, Arnett D, Moss AJ, Seidman CE, Young JB; American Heart Association; Council on Clinical Cardiology, Heart Failure and Transplantation Committee; Quality of Care and Outcomes Research and Functional Genomics and Translational Biology Interdisciplinary Working Groups; Council on Epidemiology and Prevention. Contemporary definitions and classification of the cardiomyopathies: an American Heart Association Scientific Statement from the Council on Clinical Cardiology, Heart Failure and Transplantation Committee; Quality of Care and Outcomes Research and Functional Genomics and Translational Biology Interdisciplinary Working Groups; and Council on Epidemiology and Prevention. *Circulation*. 2006;113:1807–1816.
2. Maron BJ, Gardin JM, Flack JM, Gidding SS, Kurosaki TT, Bild DE. Prevalence of hypertrophic cardiomyopathy in a general population of young adults. Echocardiographic analysis of 4111 subjects in the CARDIA Study. Coronary Artery Risk Development in (Young) Adults. *Circulation*. 1995;92:785–789.
3. Sedaghat-Hamedani F, Haas J, Zhu F, Geier C, Kayvanpour E, Liss M, Lai A, Frese K, Pribe-Wolferts R, Amr A, Li DT, Samani OS, Carstensen A, Bordalo DM, Müller M, Fischer C, Shao J, Wang J, Nie M, Yuan L, Haßfeld S, Schwartz C, Zhou M, Zhou Z, Shu Y, Wang M, Huang K, Zeng Q, Cheng L, Fehlmann T, Ehlermann P, Keller A, Dieterich C, Streckfuß-Bömeke K, Liao Y, Gotthardt M, Katus HA, Meder B. Clinical genetics and outcome of left ventricular non-compaction cardiomyopathy. *Eur Heart J*. 2017;38:3449–3460 .
4. Dong X, Fan P, Tian T, Yang Y, Xiao Y, Yang K, Liu Y, Zhou X. Recent advancements in the molecular genetics of left ventricular noncompaction cardiomyopathy. *Clin Chim Acta*. 2017;465:40–44.
5. Towbin JA, Lorts A, Jefferies JL. Left ventricular non-compaction cardiomyopathy. *Lancet*. 2015;386:813–825.
6. Hoedemaekers YM, Caliskan K, Majoor-Krakauer D, van de Laar I, Michels M, Witsenburg M, ten Cate FJ, Simoons ML, Dooijes D. Cardiac beta-myosin heavy chain defects in two families with non-compaction cardiomyopathy: linking non-compaction to hypertrophic, restrictive, and dilated cardiomyopathies. *Eur Heart J*. 2007;28:2732–2737.
7. Klaassen S, Probst S, Oechslin E, Gerull B, Krings G, Schuler P, Greutmann M, Hürlimann D, Yegitbasi M, Pons L, Gramlich M, Drenckhahn JD, Heuser A, Berger F, Jenni R, Thierfelder L. Mutations in sarcomere protein genes in left ventricular noncompaction. *Circulation*. 2008;117:2893–2901.
8. Monserrat L, Hermida-Prieto M, Fernandez X, Rodríguez I, Dumont C, Cazón L, Cuesta MG, Gonzalez-Juanatey C, Peteiro J, Alvarez N, Penas-Lado M, Castro-Beiras A. Mutation in the alpha-cardiac actin gene associated with apical hypertrophic cardiomyopathy, left ventricular non-compaction, and septal defects. *Eur Heart J*. 2007;28:1953–1961.
9. Chang B, Nishizawa T, Furutani M, Fujiki A, Tani M, Kawaguchi M, Ibuki K, Hirono K, Taneichi H, Uese K, Onuma Y, Bowles NE, Ichida F, Inoue H, Matsuoka R, Miyawaki T; Noncompaction study collaborators. Identification of a novel TPM1 mutation in a family with left ventricular noncompaction and sudden death. *Mol Genet Metab*. 2011;102:200–206.
10. Ripoll Vera T, Monserrat Iglesias L, Hermida Prieto M, Ortiz M, Rodriguez Garcia I, Govea Callizo N, Gómez Navarro C, Rosell Andreo J, Gámez Martínez JM, Pons Lladó G, Cremer Luengos D, Torres Marqués J. The R820W mutation in the MYBPC3 gene, associated with hypertrophic cardiomyopathy in cats, causes hypertrophic cardiomyopathy and left ventricular non-compaction in humans. *Int J Cardiol*. 2010;145:405–407.
11. Sadeghpour A, Faghihi S, Alizadehasl A. Can hypertrophic cardiomyopathy and non compaction left ventricle coexist in a single patient? *Int J Cardiovasc Imaging*. 2015;31:319–321.
12. Baker ML, Fong MW, Goldman B. Hypertrophic cardiomyopathy with features of left ventricular non-compaction: how many diseases? *Int J Cardiol*. 2011;148:364–366.
13. Yuan L, Xie M, Cheng TO, Wang X, Zhu F, Kong X, Ghoorah D. Left ventricular noncompaction associated with hypertrophic cardiomyopathy: echocardiographic diagnosis and genetic analysis of a new pedigree in China. *Int J Cardiol*. 2014;174:249–259.
14. Pua CJ, Bhalshankar J, Miao K, Walsh R, John S, Lim SQ, Chow K, Buchan R, Soh BY, Lio PM, Lim J, Schafer S, Lim JQ, Tan P, Whiffin N, Barton PJ, Ware JS, Cook SA. Development of a comprehensive sequencing assay for inherited cardiac condition genes. *J Cardiovasc Transl Res*. 2016;9:3–11.
15. Schymkowitz JW, Rousseau F, Martins IC, Ferkinghoff-Borg J, Stricher F, Serrano L. Prediction of water and metal binding sites and their affinities by using the Fold-X force field. *Proc Natl Acad Sci USA*. 2005;102:10147–10152.
16. Jenni R, Oechslin E, Schneider J, Attenhofer Jost C, Kaufmann PA. Echocardiographic and pathoanatomical characteristics of isolated left ventricular noncompaction: a step towards classification as a distinct cardiomyopathy. *Heart*. 2001;86:666–671.
17. Olson TM, Michels VV, Thibodeau SN, Tai YS, Keating MT. Actin mutations in dilated cardiomyopathy, a heritable form of heart failure. *Science*. 1998;280:750–752.
18. Olson TM, Doan TP, Kishimoto NY, Whitby FG, Ackerman MJ, Fananapazir L. Inherited and de novo mutations in the cardiac actin gene cause hypertrophic cardiomyopathy. *J Mol Cell Cardiol*. 2000;32:1687–1694.
19. Mogensen J, Klausen IC, Pedersen AK, Egeblad H, Bross P, Kruse TA, Gregersen N, Hansen PS, Baandrup U, Borglum AD. Alpha-cardiac actin is a novel disease gene in familial hypertrophic cardiomyopathy. *J Clin Invest*. 1999;103:R39–R43.
20. Van Driest SL, Ellsworth EG, Ommen SR, Tajik AJ, Gersh BJ, Ackerman MJ. Prevalence and spectrum of thin filament mutations in an outpatient referral population with hypertrophic cardiomyopathy. *Circulation*. 2003;108:445–451.
21. Tian T, Wang J, Wang H, Sun K, Wang Y, Jia L, Zou Y, Hui R, Zhou X, Song L. A low prevalence of sarcomeric gene variants in a Chinese cohort with left ventricular non-compaction. *Heart Vessels*. 2015;30:258–264.
22. Matsson H, Eason J, Bookwalter CS, Klar J, Gustavsson P, Sunnegårdh J, Enell H, Jonzon A, Vikkula M, Gutierrez I, Granados-Riveron J, Pope M, Bu'Lock F, Cox J, Robinson TE, Song F, Brook DJ, Marston S, Trybus KM, Dahl N. Alpha-cardiac actin mutations produce atrial septal defects. *Hum Mol Genet*. 2008;17:256–265.

23. Greenway SC, McLeod R, Hume S, Roslin NM, Alvarez N, Giuffre M, Zhan SH, Shen Y, Preuss C, Andelfinger G; FORGE Canada Consortium, Jones SJ, Gerull B. Exome sequencing identifies a novel variant in ACTC1 associated with familial atrial septal defect. *Can J Cardiol*. 2014;30:181–187.
24. Taylor M, Graw S, Sinagra G, Barnes C, Slavov D, Brun F, Pinamonti B, Salcedo EE, Sauer W, Pyxaras S, Anderson B, Simon B, Bogomolovas J, Labeit S, Granzier H, Mestroni L. Genetic variation in titin in arrhythmogenic right ventricular cardiomyopathy-overlap syndromes. *Circulation*. 2011;124:876–885.
25. Maron MS, Rowin EJ, Appelbaum E, Chan RH, Gibson CM, Lesser JR, Lindberg J, Haas TS, Udelson JE, Manning WJ, Maron BJ. Prevalence and clinical profile of myocardial crypts in hypertrophic cardiomyopathy. *Circ Cardiovasc Imaging*. 2012;5:441–447.
26. Johansson B, Maceira AM, Babu-Narayan SV, Moon JC, Pennell DJ, Kilner PJ. Clefts can be seen in the basal inferior wall of the left ventricle and the left interventricular septum in healthy volunteers as well as patients by cardiovascular magnetic resonance. *J Am Coll Cardiol*. 2007;50:1294–1295.
27. Teare D. Asymmetrical hypertrophy of the heart in young adults. *Br Heart J*. 1958;20:1–8.
28. Kuribayashi T, Roberts WC. Myocardial disarray at junction of ventricular septum and left and right ventricular free walls in hypertrophic cardiomyopathy. *Am J Cardiol*. 1992;70:1333–1340.
29. Whittaker P, Romano T, Silver MD, Boughner DR. An improbe method for detecting and quantifying cardiac muscle disarray in hypertrophic cardiomyopathy. *Am Heart J*. 1989;118:341–346.

SUPPLEMENTAL MATERIAL

Table S1. Alignment of amino acid residues adjacent to ACTC1 p.(Ala21Val) sequence variant showing level of conservation among different species.

Homo Sapiens	1	MCDDEETTALVCDNGSGLVK**A**GFAGDDAPRAVFPSIVGRPRHQGVMVGMG	50
Pan troglodytes	1	MCDDEETTALVCDNGSGLVK**A**GFAGDDAPRAVFPSIVGRPRHQGVMVGMG	50
Macaca Mulatta	1	MCDDEETTALVCDNGSGLVK**A**GFAGDDAPRAVFPSIVGRPRHQGVMVGMG	50
Canis lupus familiaris	1	MCDDEETTALVCDNGSGLVK**A**GFAGDDAPRAVFPSIVGRPRHQGVMVGMG	50
Bos taurus	1	MCDDEETTALVCDNGSGLVK**A**GFAGDDAPRAVFPSIVGRPRHQGVMVGMG	50
Mus musculus	1	MCDDEETTALVCDNGSGLVK**A**GFAGDDAPRAVFPSIVGRPRHQGVMVGMG	50
Rattus norvegicus	1	MCDDEETTALVCDNGSGLVK**A**GFAGDDAPRAVFPSIVGRPRHQGVMVGMG	50
Gallus gallus	1	MCDDEETTALVCDNGSGLVK**A**GFAGDDAPRAVFPSIVGRPRHQGVMVGMG	50
Danio rerio	1	MCDDDETTALVCDNGSGLVK**A**GFAGDDAPRAVFPSIVGRPRHQGVMVGMG	50
Arabidopsis thaliana	1	MADGEDIQPLVCDNGTGMVK**A**GFAGDDAPRAVFPSIVGRPRHTGVMVGMG	50
Oryza sativa Japonica Group	1	MADGEDIQPLVCDNGTGMVK**A**GFAGDDAPRAVFPSIVGRPRHTGVMVGMG	50
Xenopus tropicalis	1	MCDDEETTALVCDNGSGLVK**A**GFAGDDAPRAVFPSIVGRPRHQGVMVGMG	50

The amino acidic residue altered by the mutation is is shown in red (*Homo sapiens* [NP_005150.1], *pan troglodytes* [XP_510285.1], *macaca mulatta* [XP_001088409.2], *canis lupus familiaris* [XP_535424.1], *bos taurus* [NP_001029757.1], *mus musculus* [NP_033738.1], *rattus norvegicus* [NP_062056.1], *gallus gallus* [NP_001072949.1], *danio rerio* [NP_001001409.2], *arabidopsis thaliana* [NP_196543.1], *oryza sativa japonica group* [NP_001065830.1], *xenopus tropicalis* [NP_989094.1]).